



# Sensitivity analysis of gravity anomalies and vertical gravity gradient data for bathymetry inversion

Xiaoyun Wan<sup>1,2</sup> · Jiangjun Ran<sup>3</sup> · Shuanggen Jin<sup>4</sup>

Received: 16 January 2018 / Accepted: 31 May 2018 / Published online: 6 June 2018  
© Springer Nature B.V. 2018

## Abstract

Bathymetry is the measurement of the water depth similar to underwater topography. Gravity anomaly and vertical gravity gradient are important data used to inverse bathymetry. In this study, we investigate the sensitivities of the gravity anomalies and vertical gravity gradient data to bathymetry inversion. Firstly, the formulas of the gravity anomaly and vertical gravity gradient signals produced by the seabed terrain are derived, and then a series of numerical studies are designed to investigate the sensitivities. The results show that gravity anomalies and vertical gravity gradients have different sensitive bands to bathymetry inversion. Therefore, accuracy requirements for the gravity anomaly and vertical gravity gradient data are different for bathymetry inversion with different spatial resolutions and accuracies. With decreasing resolution, the accuracy requirement of the gravity anomaly gradually decreases, whereas the accuracy requirement of the vertical gravity gradient first decreases and then increases, indicating that the vertical gravity gradient is more sensitive to the short-wavelength signal than the gravity anomaly, especially in the 0–20 km wavelength ranges. In addition, we perform a theoretical analysis that shows that the vertical gravity gradient has a band that is most sensitive to the seafloor topography. This study is capable to provide a reference for the design of future satellites to retrieve the bathymetry.

**Keywords** Gravity anomaly · Vertical gravity gradient · Bathymetry inversion · Accuracy requirement · Seafloor topography

## Introduction

Bathymetry information is of great importance for many purposes, e.g., navigation, security, coastal zone management, and etc. Using the gravity anomalies and vertical gravity gradients derived from altimetry observations to inverse bathymetry is one of the effective methods for obtaining bathymetry information. Many previous studies

(Calmant 1994; Smith and Sandwell 1997; Hwang 1999; Wang et al. 2001; Jena et al. 2012; Ouyang et al. 2014; Hu et al. 2014a, b; Hsiao et al. 2016) have investigated corresponding algorithms and obtained bathymetry grids, such as ETOPO1, SRTM30\_PLUS and GEBCO\_2014 Grid. New altimetry satellite missions, such as the Surface Water and Ocean Topography (SWOT) mission (Fu et al. 2012), is capable to provide observations with higher spatial resolution and accuracy. A previous study suggested that the seafloor topography with a wavelength between 2 and 12 km can be determined using vertical gravity gradient data (Sandwell et al. 2014a). The studies above indicate that gravity anomalies and vertical gravity gradients are useful for deriving ocean bottom topography. Gravity anomalies are the differences between the gravity observations at the geoid surface and the values at the ellipsoid surface from the normal gravity field model (Moritz 2005). Gravity gradients are the spatial ratio of changes of gravity. These two types of data can be derived from gravity satellites and altimetry satellite observations (Rummel and Haagmans 1990; Bao et al. 2013). Especially with the advent of satellite altimetry,

---

✉ Jiangjun Ran  
jiangjunran@gmail.com

✉ Shuanggen Jin  
sgjin@shao.ac.cn

<sup>1</sup> Qian Xuesen Laboratory of Space Technology,  
Beijing 100094, China

<sup>2</sup> China University of Geosciences, Beijing 100083, China

<sup>3</sup> Delft University of Technology, Stevinweg 1, 2628 CN Delft,  
The Netherlands

<sup>4</sup> Shanghai Astronomical Observatory, Chinese Academy  
of Sciences, Shanghai 200030, China

vertical deflections can be derived from altimeter observations, and then gravity anomalies can be calculated by Inverse Vening Meinesz formula (Hwang 1998). The vertical gravity gradient can be obtained by method of Rumel and Haagmans (1990) with vertical deflections from altimetry observations. Definitely, the anomalies in gravity and gravity gradients are partly from the bathymetry information. This is why we can use gravity anomalies and vertical gravity gradients to predict the bathymetry. Hence, we need satellite observations to obtain gravity anomalies and vertical gravity gradients data, which are further used to derive the information of bathymetry. However, in order to design some new satellites, we need to first know what the accuracy requirements of the gravity anomalies and vertical gravity gradients for bathymetry inversion are. This is the starting point of this paper.

Sandwell et al. (2006) found that a unit Bouguer layer with a thickness of 1 km creates 70 mgal gravity anomaly. Many other investigators have examined the sensitive bands of geoid and gravity anomaly to derive seafloor topography. For example, Dixon and Naraghi (1983) reported a strong correlation in the 50–300 km wavelength range between the geoid and bathymetry, and other studies (Sandwell et al. 2006, 2014a; Hwang 1999; Hu et al. 2014a, b) reported that gravity anomalies have a strong correlation with bathymetry in the 20–200 km wavelength range. The isostatic compensation will mainly contribute the long-wavelengths of the gravity anomalies, which can be filtered by high-pass filters (Sandwell et al. 2001) or can be modelled by some ship-depths observations (Kim et al. 2011; Xiang et al. 2017). Furthermore, many reports (Calmant and Baudry 1996; Sandwell et al. 2001; Kim et al. 2010; Xiang et al. 2017) have pointed out that the accuracy of gravity anomaly measurements influences the accuracy of bathymetry inversions. However, only few studies (Sandwell et al. 2006) have discussed gravity anomaly accuracy requirements, in order to obtain the bathymetry information with a given accuracy.

Currently, besides gravity anomalies as discussed above, it becomes possible to derive vertical gravity gradients using satellite altimetry observations (Sandwell et al. 2014a), particularly due to the high spatial resolution of synthetic aperture radar (SAR) and interferometric synthetic aperture radar (InSAR) altimeters (Fu et al. 2012; Bao et al. 2013; Sui et al. 2017). In Wang (2000), a least-squares method was firstly proposed to estimate a bathymetry model using a vertical component of gravity gradients. Furthermore, a research adopted a non-linear least-squares algorithm to estimate the position of a seamount from a satellite-derived vertical gravity gradient (Kim and Wessel 2015). The research pointed out that the signal-to-noise ratio of the new vertical gravity gradients has been improved and the data give us better opportunities to find small seamounts. Some studies (Hu et al. 2014a, b)

derived bathymetry using vertical gravity gradient data provided by the Scripps Institute of Oceanography (SIO) and concluded that the accuracy of bathymetry prediction can be improved by combining the vertical gravity gradient and gravity anomaly data. However, the accuracy requirements of determining bathymetry from vertical gravity gradients are still unknown.

The sensitivities of gravity anomalies and vertical gravity gradients to retrieve the seafloor topography at various spatial resolutions are different. Therefore, accuracy requirements of gravity anomaly and vertical gravity gradient should be different, if the target spatial resolution and accuracy of the bathymetry inversion are different. In this paper, the sensitivity and accuracy requirements of gravity anomaly and vertical gravity gradient data for bathymetry inversion are analyzed in order to provide a reference for the design of new gravity satellites and altimetry satellites. In “Theory and method” section, the formulas of the gravity anomaly and vertical gravity gradient generated from the seafloor topography are derived, the accuracy requirements using numerical analysis are presented in “Numerical results and analysis” section, discussion is given in “Discussion” section, and finally the conclusions are given in “Conclusions” section.

## Theory and method

Seafloor topography can be represented by an average elevation of its upper surface, and a cylinder can be used to represent the topographic relief in a local area, as shown in Fig. 1.

To derive the gravity anomaly produced by the cylinder, the local coordinate system shown in Fig. 2 is set up. The solution is derived in cylindrical coordinates for the observation point, denoted as  $P$ , located at the origin above the cylinder.

Where point  $P$  is on the sea surface,  $H$  is the depth of the datum plane,  $h$  denotes the water depth at point  $P$  and  $a$  is the radius of the cylinder. Thus, the gravity anomaly created by

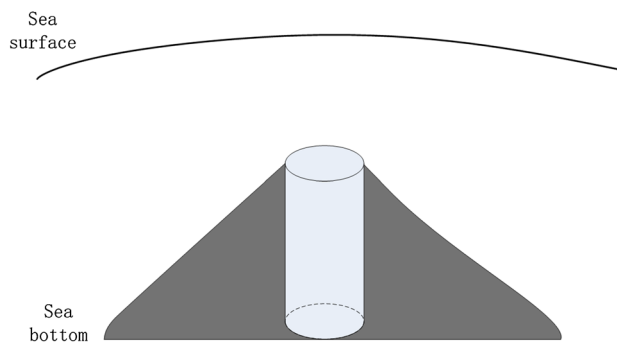


Fig. 1 Sketch of seafloor topography

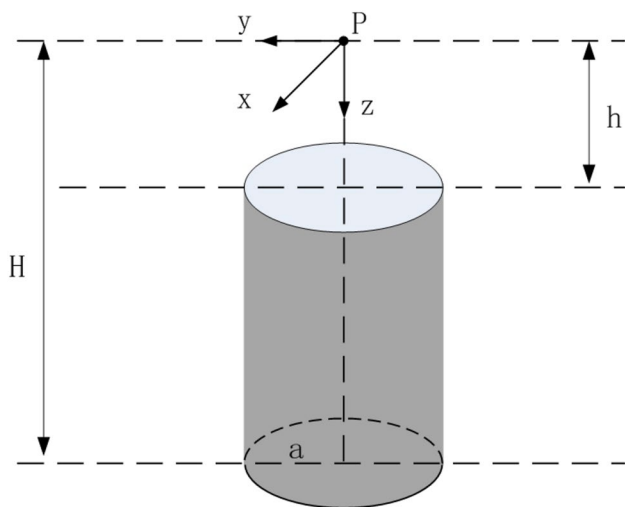


Fig. 2 Sketch of the cylinder

the cylinder at point *P* can be expressed as (Kim and Wessel 2016):

$$\begin{aligned}
 g_z &= \int_0^{2\pi} d\theta \int_h^H \int_0^a \frac{G\rho zr}{(r^2 + z^2)^{\frac{3}{2}}} dr dz \\
 &= 2\pi G\rho \int_h^H z \left( -\frac{1}{\sqrt{r^2 + z^2}} \right) \Big|_{r=0}^{r=a} dz \\
 &= 2\pi G\rho \left[ (H - h) - \left( \sqrt{a^2 + z^2} \right) \Big|_{z=h}^{z=H} \right] \\
 &= 2\pi G\rho(H - h) - 2\pi G\rho \left( \sqrt{a^2 + H^2} - \sqrt{a^2 + h^2} \right)
 \end{aligned} \tag{1}$$

where *G* is the gravitational constant,  $\rho$  is the density of the cylinder and *r* is the horizontal distance from the integral element to the origin, i.e.,  $r = \sqrt{x^2 + y^2}$  where  $x = r \cos \theta$ ,  $y = r \sin \theta$ . Definitely, the direction of  $g_z$  is same as the direction of *Z* axis. In Eq. (1), when *a* is large, the non-linear term can be neglected as follows:

$$g_z = 2\pi G\rho(H - h) \tag{2}$$

If we know  $g_z$ , by solving formula (2), we can obtain *h*. This method is so called the gravity-geologic method (GGM) (Ibrahim and Hinze 1972; Kim et al. 2011), which has been used in several studies to determine the seafloor topography (Kim et al. 2011; Hsiao et al. 2011, 2016).

Similarly, the vertical component of the gravity gradient at point *P* can be expressed as:

$$\begin{aligned}
 g_{zz} &= \int_0^{2\pi} d\theta \int_h^H \int_0^a \left( \frac{G\rho}{(r^2 + z^2)^{\frac{3}{2}}} - \frac{3Gz^2\rho}{(r^2 + z^2)^{\frac{5}{2}}} \right) r dr dz \\
 &= 2\pi G\rho \int_0^a r \frac{z}{(r^2 + z^2)^{\frac{3}{2}}} \Big|_{z=h}^{z=H} dr \\
 &= 2\pi G\rho \left( \frac{-H}{(H^2 + r^2)^{\frac{1}{2}}} + \frac{h}{(h^2 + r^2)^{\frac{1}{2}}} \right) \Big|_{r=0}^{r=a} \\
 &= 2\pi G\rho \left( \frac{-H}{(H^2 + a^2)^{\frac{1}{2}}} + \frac{h}{(h^2 + a^2)^{\frac{1}{2}}} \right)
 \end{aligned} \tag{3}$$

In theory, this formula can be used for seafloor topography inversion and parameters  $\rho$  and *a* can be determined using an iteration method as the GGM (Kim et al. 2011; Ouyang et al. 2014). Because seafloor topography inversion is out of the scope of this research, we will not discuss how to obtain *h* here.

## Numerical results and analysis

### Gravity anomaly for bathymetry inversion

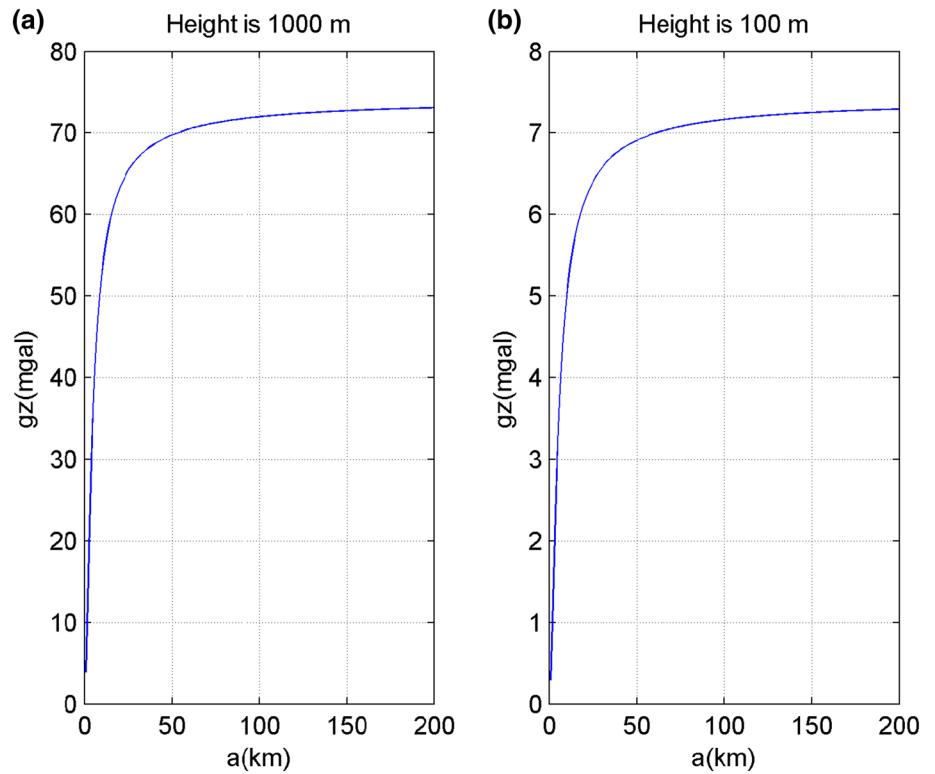
When discussing the gravity anomaly produced by seafloor topography, the parameter  $\rho$  in Eqs. (1)–(3) needs to be changed as  $\Delta\rho$ , which represents the density difference between the rock and the seawater in the area where the terrain is addressed. If the average density of the seafloor rock is  $\rho_r = 2800 \text{ kg/m}^3$  and the average density of seawater is  $\rho_s = 1030 \text{ kg/m}^3$  (Sandwell et al. 2001), the gravity signal at the sea surface produced by per km of the Bouguer layer is approximated as:

$$g_z = 2\pi G\Delta\rho\Delta H = 74.2 \text{ mgal} \tag{4}$$

where  $\Delta\rho = \rho_r - \rho_s$  and  $\Delta H = 1 \text{ km}$ . If the depth of the reference surface is chosen as the mean water depth, i.e.  $H = 3.5 \text{ km}$ , the variation of the gravity anomaly as a function of the cylinder radius *a* is shown in Fig. 3a, where the height of the cylinder is 1 km. If the height of the seafloor topography is 100 m, the gravity anomaly created by the corresponding cylinder is shown in Fig. 3b.

According to Fig. 3b, the gravity anomaly is approximately 7.3 mgal when the radius of the cylinder is larger than 50 km. Hence, if the accuracy requirement for

**Fig. 3** Gravity anomalies created by cylinder with different radius. **a** Height of the cylinder is 1 km. **b** Height of the cylinder is 100 m



bathymetry inversion is 100 m when the spatial resolution is  $1^\circ \times 1^\circ$  ( $1^\circ$  corresponds to 110 km at Earth’s equator), the accuracy requirement for the gravity anomaly is 7.3 mgal because only when the observation error is smaller than the signal, the signal can be extracted. If we assume that the spatial resolution and accuracy of estimated bathymetry are  $\Delta\theta \times \Delta\theta$ ,  $\delta_h$ , respectively, without considering the effect of the inversion computing error, the minimum requirement for the accuracy of the gravity data can be simplified as follows:

$$\begin{aligned} \delta_{g_z} &= 2\pi G\rho\delta_h - 2\pi G\rho\left(\sqrt{a^2 + H^2} - \sqrt{a^2 + (H - \delta_h)^2}\right) \\ &= 2\pi G\rho\delta_h - 2\pi G\rho\frac{(2H - \delta_h)\delta_h}{\sqrt{a^2 + (H - \delta_h)^2} + \sqrt{a^2 + H^2}} \end{aligned} \tag{5}$$

where  $a = R\Delta\theta/2$ . Here, the minimum requirement is the magnitude of the gravity signal generated by seafloor topography with a height of  $\delta_h$ . According to Eq. (5), the magnitude of  $\delta_{g_z}$  is not only related to  $\delta_h$  but also to  $a$  and  $H$ , where  $a$  reflects the size of the terrain area, which represents the target spatial resolution of inversion. The parameter  $H$  refers to the bottom depth of the corresponding cylinder.

As shown in Fig. 4, the accuracy requirements of the gravity anomaly decrease with respect to a decrease in the spatial resolution ( $a$  becomes larger). The accuracy requirements of gravity anomalies are different when

seafloor topographies are located at different depths. The deeper the depth is, the higher the accuracy requirement of a gravity anomaly is, since the signal would be considerably weak if the topography was located at a great depth in the sea. To determine the average gravity anomaly accuracy requirements for a global seafloor topography inversion, assuming that the target inversion accuracy is 100 m for a 3.5 km mean depth, Table 1 lists the minimum accuracy requirements of gravity observations for different spatial resolutions.

According to Sandwell et al. (2014b), the gravity anomaly accuracy provided by altimetry satellites has reached 2 mgal. Therefore, according to Table 1, the altimetry satellite gravity anomaly product can retrieve seafloor topography information at the spatial resolution of 7.2 km (7.2 km corresponds to 4’ in Table 1) with an accuracy of 100 m. To retrieve higher accuracy and higher resolution of the seafloor topography data, higher accuracy and higher resolution gravity anomaly products are required, i.e., new satellites, equipped with more accurate sensors to provide these products, are needed.

**Vertical gravity gradient for bathymetry inversion**

When discussing the gradient anomalies caused by the seafloor topography, the parameter  $\rho$  in Eq. (3) should also be changed as  $\Delta\rho$  like in Eq. (4). According to Eq. (3), the vertical gravity

**Fig. 4** Variations of the gravity anomaly with different depth references and resolutions when the accuracy of bathymetry inversion is 100 m

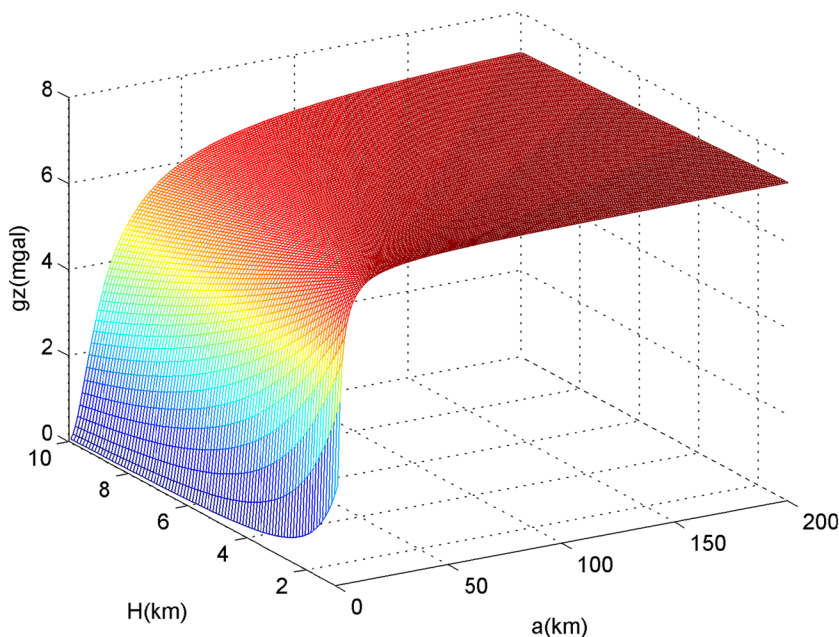


**Table 1** The minimal accuracy requirement of the gravity anomaly when the target accuracy of the topography inversion is 100 m

$\Delta\theta$	a (km)	$\delta_{\Delta g}$ (mgal)
1'	0.9	0.3
2'	1.9	0.9
3'	2.8	1.6
4'	3.7	2.4
5'	4.6	3.0
6'	5.6	3.5
7'	6.5	3.9
8'	7.4	4.3
9'	8.3	4.6
10'	9.3	4.8

gradients generated by cylinders with a height of 1 km at a mean depth of 3.5 km are shown in Fig. 5.

Figure 5 shows that the absolute values of the vertical gravity gradients first increase, then decrease with respect to an increase in the radius of the cylinder. In addition, we found that when  $a$  is smaller than 50 km, the absolute value of the vertical gravity gradient is usually larger than that when  $a$  is larger than 50 km, indicating that the vertical gravity gradient is more sensitive to the local signal, compared with gravity anomaly. We also found that there is a turning point in the variation of the vertical gravity gradient. To calculate the value of  $a$  at the turning point, we set

$$f(a) = 2\pi G\Delta\rho \left( \frac{-H}{(H^2 + a^2)^{\frac{1}{2}}} + \frac{h}{(h^2 + a^2)^{\frac{1}{2}}} \right) \tag{6}$$

Then,

$$\frac{\partial f}{\partial a} = -2\pi G\Delta\rho \left( \frac{-H}{(H^2 + a^2)^{\frac{3}{2}}} + \frac{h}{(h^2 + a^2)^{\frac{3}{2}}} \right) \tag{7}$$

The value of  $a$  at the turning point can be obtained by solving  $\partial f/\partial a = 0 (a > 0)$  as follows:

$$a = H^{\frac{1}{3}} h^{\frac{1}{3}} \sqrt{H^{\frac{2}{3}} + h^{\frac{2}{3}}} \tag{8}$$

Hence, the corresponding vertical gravity gradient can be expressed as follows:

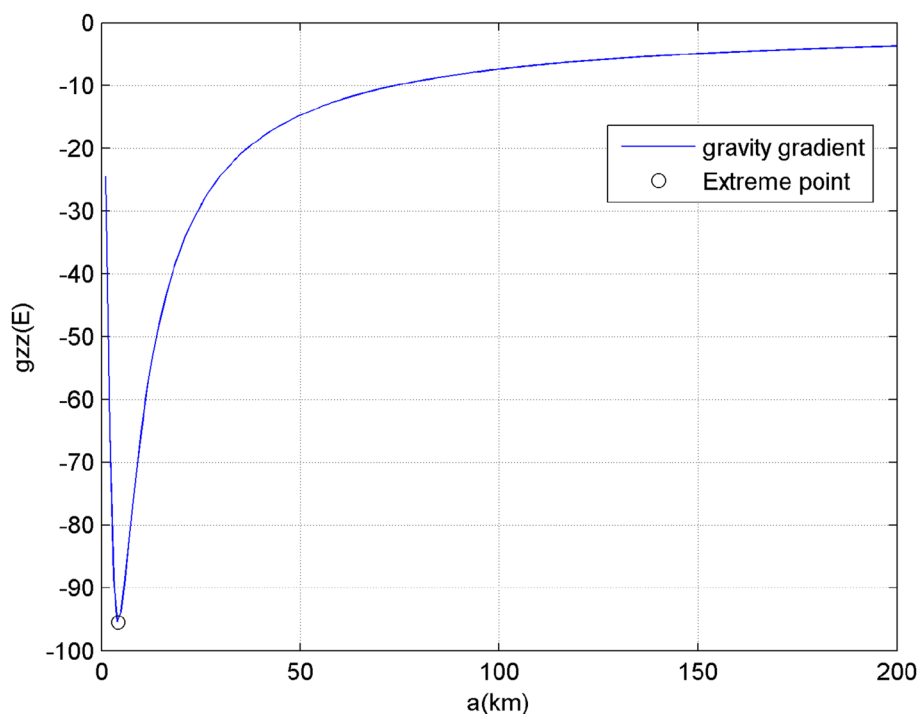
$$f(a)_e = 2\pi G\Delta\rho \left( \frac{-H}{\left( H^2 + H^{\frac{2}{3}} h^{\frac{2}{3}} \left( H^{\frac{2}{3}} + h^{\frac{2}{3}} \right) \right)^{\frac{1}{2}}} + \frac{h}{\left( h^2 + H^{\frac{2}{3}} h^{\frac{2}{3}} \left( H^{\frac{2}{3}} + h^{\frac{2}{3}} \right) \right)^{\frac{1}{2}}} \right) \tag{9}$$

The coordinates of the extreme points in Fig. 5 are calculated using Eqs. (8) and (9), and we get  $a = 4.2$  km and  $f(a)_e = -95.5$  E ( $1 \text{ E} = 10^{-9} \text{ s}^{-2}$ ).

The turning point in Fig. 5 indicates that a 1 km high topographic relief at a depth of 3.5 km with an undulating area radius of 4.2 km will produce a gravity gradient with a value of  $-95.5$  E at the sea surface. The magnitude of the signal is sufficiently large to be observed by current gravity gradiometers and is expected to be detected by new



**Fig. 5** Variations of the vertical gravity gradient with the radius of the cylinder (assuming that the height of the cylinder is 1 km)



satellite altimeter products. However, if the area is considerably large, the vertical gravity gradient signal generated at the sea surface would be considerably weak due to the low signal-to-noise ratio, thereby making it difficult to detect the signal. It can be concluded from Fig. 5 that for 1 km high seabed topography at a depth of 3.5 km, the most sensitive half-band wavelength by the vertical gravity gradient is 4.2 km. This is consistent with the findings of Sandwell et al. (2014a), i.e. a 2–12 km scale topography variation can be observed using the vertical gravity gradient.

At this point, we conclude that the vertical gravity gradient is more sensitive to short-wavelength seafloor topography. In particular, for a specific depth and specific height topography variation, there exists a most sensitive band. The size of the band can be calculated using Eq. (8), and the corresponding signal values can be obtained using Eq. (9). Compared to gravity anomalies, the superiority of vertical gravity gradients is approximately 0–20 km in the wavelength (Figs. 3, 5). To further illustrate this finding, we calculate the value of the vertical gravity gradient created by a 100 m high cylinder with different depths and radii (corresponding to different resolution), as shown in Fig. 6. It is evident from this figure that the signal becomes stronger when the water becomes shallower. With the increase of  $a$ , the absolute value of the vertical gravity gradient signal first increases and then decreases. Certainly, the stronger the signal is, the easier it is to detect it. Hence, the vertical gravity gradient is more sensitive to the short-wavelength signal than the gravity anomaly.

Similarly, we consider the intensity of the signal as the minimum requirement for the accuracy of the vertical gravity gradient data. If the target inversion resolution is  $\Delta\theta \times \Delta\theta$  and accuracy is  $\delta_h$ , without considering the effect of the inversion computing error, the minimum requirement for the accuracy of the vertical gravity gradient data can be expressed as follows:

$$\delta_{g_{zz}} = 2\pi G\Delta\rho \left( \frac{-H}{(H^2 + a^2)^{\frac{1}{2}}} + \frac{H - \delta_h}{((H - \delta_h)^2 + a^2)^{\frac{1}{2}}} \right) \quad (10)$$

Considering the inversion of the topography at the mean water depth as an example, if the accuracy requirement is 100 m, Table 2 lists the minimum gravity gradient accuracy requirement with the variation of  $\Delta\theta$ .

## Discussion

According to the analysis above, in order to invert bathymetry with high accuracy, we need accurate gravity anomalies and gravity gradients. In order to show the accuracy of the current gravity field products, we estimate the accuracies of vertical deflections ( $\delta_\epsilon$  and  $\delta_\eta$ ), gravity anomalies calculated by the ultra high degree gravity field models provided by German Research Centre for Geosciences (GFZ). High resolution is one of the main requirements to gravity field products for bathymetry inversion. Hence, we only select models

**Fig. 6** Variation in vertical gravity gradient with different depth references and resolutions when the accuracy of bathymetry inversion is 100 m

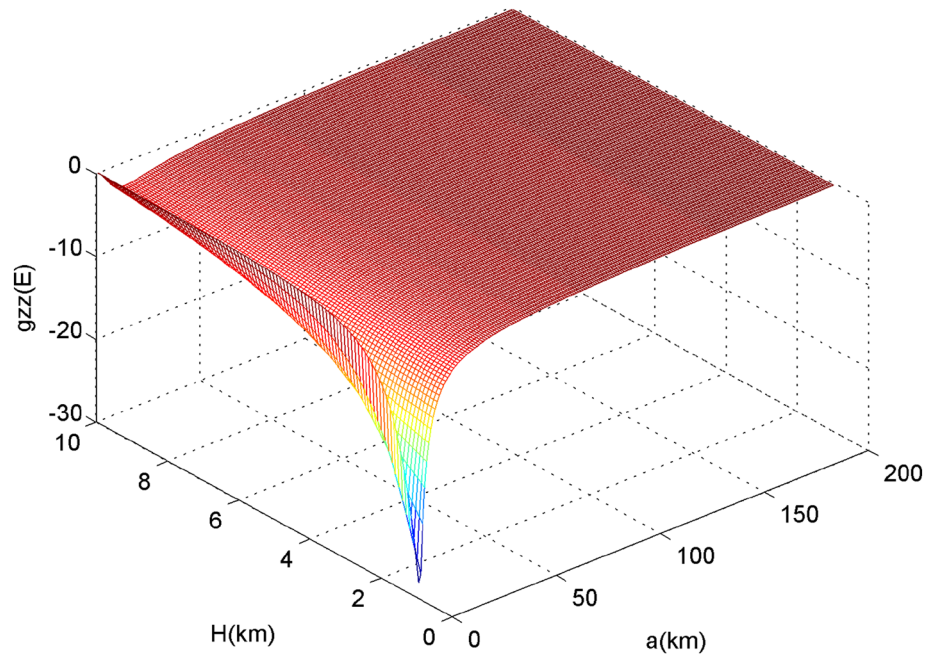


**Table 2** The minimal gravity gradient accuracy requirements when the target accuracy of the topography inversion is 100 m

$\Delta\theta$	a (km)	$\delta_{g_{zz}}$ (E)
1'	0.9	1.4
2'	1.9	4.2
3'	2.8	6.6
4'	3.7	7.9
5'	4.6	8.3
6'	5.6	8.2
7'	6.5	7.9
8'	7.4	7.5
9'	8.3	7.0
10'	9.3	6.6

whose maximum degrees are larger than 1000 in this analysis, including EGM08, EIGEN6C, EIGEN6C2, EIGEN6C3, EIGEN6C4 and GECO. With the standard deviations of the coefficients provided by these models, the standard deviation of vertical deflections and gravity anomalies are calculated

on the Earth surface at grids  $1^\circ \times 1^\circ$ . Mean values of these values for each model are given in Table 3.

In Table 3,  $\delta_\epsilon$ ,  $\delta_\eta$  and  $\delta_{\Delta g}$  represents accuracies of two components of vertical deflections and gravity anomalies respectively. It can be found that errors of  $\eta$  are almost three times larger than  $\epsilon$ . This might be caused by the reason that inversion of these gravity field models all used altimetry data. When computing vertical deflections using the traditional altimetry observations, it is better to make geoid difference in the along-track to reduce the environment noises. However, the direction of the satellite track is often more close to south-north direction (e.g. HY-2A, see Fig. 7). According to this figure, the distance between trajectories on the earth surface is larger than a few hundred kilometres. Hence, in the cross-track direction, the environment noises are not easily to be reduced by the difference which will create much more noises to  $\eta$  compared to  $\epsilon$ . According to Molodensky (1960) and Wan et al. (2017), the accuracies of  $\epsilon$  and  $\eta$  has some relationship with  $\Delta g$ , i.e.,  $\delta_{\Delta g} \approx \gamma \sqrt{\delta_\epsilon^2 + \delta_\eta^2}$ .

**Table 3** Accuracy of ultrahigh degree gravity field models (the maximum degree is larger than 1000)

Model	Data source	Degree	Resolution (km)	$\delta_\epsilon$ (s)	$\delta_\eta$ (s)	$\delta_{\Delta g}$ (mgal)
EGM08	S (Grace), G, A	2190	9	0.04	0.15	9.03
EIGEN6C	S (Goce, Grace, Lageos), G, A	1420	14	0.06	0.16	5.86
EIGEN6C2	S (Goce, Grace, Lageos), G, A	1949	10	0.05	0.15	5.63
EIGEN6C3	S (Goce, Grace, Lageos), G, A	1949	9	0.04	0.11	4.29
EIGEN6C4	S (Goce, Grace, Lageos), G, A	2190	9	0.03	0.09	2.73
GECO	S (Goce), EGM08	2190	9	0.03	0.13	8.41

S satellite tracking data, G gravity data, A altimetry data

**Fig. 7** Ground track of HY-2A for 1 day

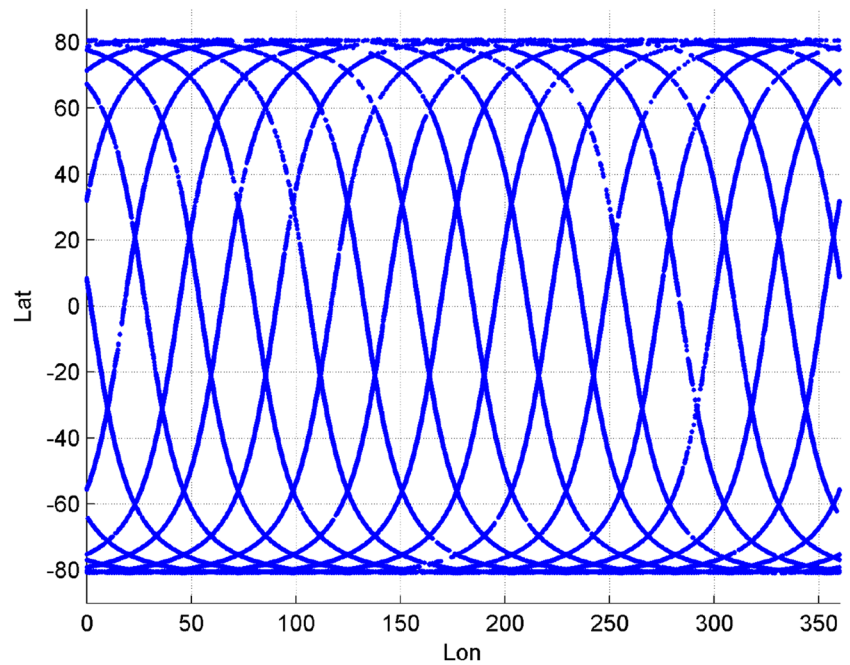
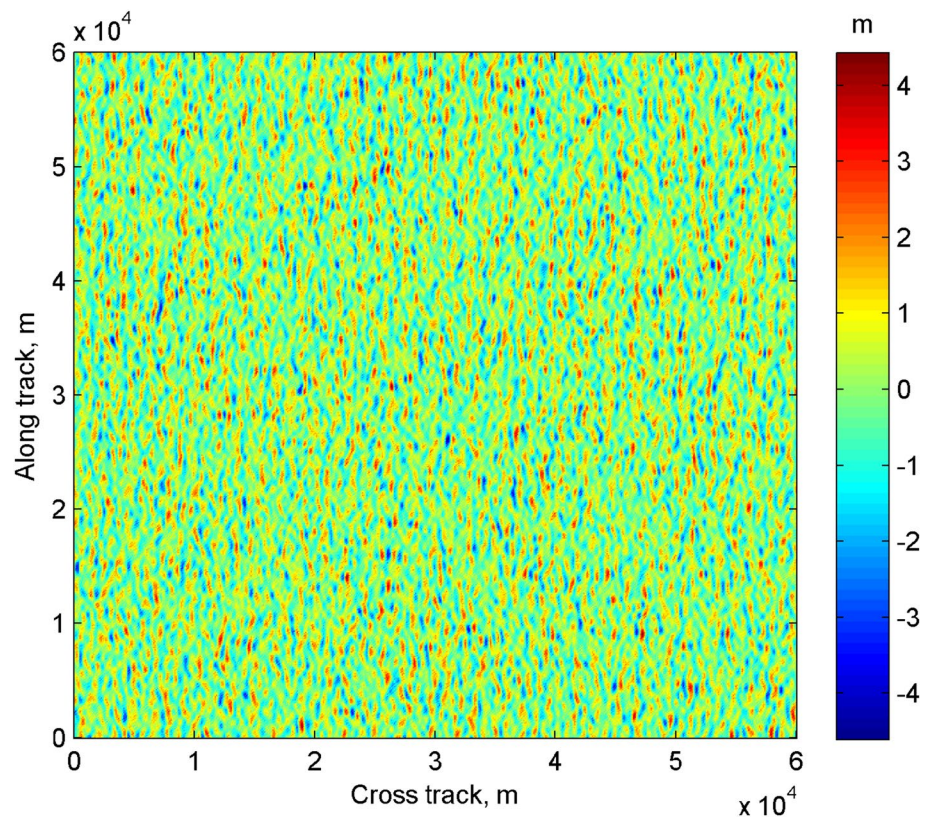


**Fig. 8** Simulated surface observed by InSAR Altimeter



Hence, if the accuracies of  $\eta$  can be improved at level as  $\varepsilon$ , the accuracy of gravity anomaly will be improved by 2 times. This may be achieved by InSAR altimetry (Fu et al. 2012; Bao et al. 2013; Sui et al. 2017), because this technique can observe two-dimensional elevation near the

ground track like in Fig. 8 (Sui et al. 2017). The accuracy of this altimeter can achieve at several centimetres (Fu et al. 2012; Sui et al. 2017), almost close to the traditional altimeter (Bao et al. 2013). Hence, with observations from this new altimeter, there will be no accuracy differences between



$\varepsilon$  and  $\eta$ , since we can conduct the difference as the same accuracy in arbitrary direction. This improvement will be favorable to the bathymetry inversion.

As for the ocean gravity gradient computing, it is necessary to use a distance which is the double difference of the geoid elevation, for example,

$$T_{xx} = \gamma \frac{\partial^2 N}{\partial x^2} \quad (11)$$

where  $\gamma$  is the normal gravity and  $\frac{\partial^2 N}{\partial x^2}$  can be obtained from the difference of  $\frac{\Delta N}{\Delta x}$ , which is the difference of the geoid elevation in the  $X$  direction. Hence, in order to obtain  $T_{xx}$ , we need the double difference of the geoid elevation. Because the sampling interval of the traditional altimeter is approximately 7 km, the two times difference requires at least three points and the corresponding distance is 14 km. According to the sampling theorem (Proakis and Manolakis 2007), the shortest wavelength gravity gradient signal that can be extracted from elevation observations is 28 km. In addition, for the traditional altimeter, it is better to make the difference in the along-track. Due to these reasons, it is difficult to obtain high-resolution and high-accuracy ocean gravity gradient data using traditional altimetry technologies. In recent years, SAR altimetry has been developed successfully (Stenseng and Andersen 2012). This altimetry has the following two benefits with respect to conventional altimetry due to its advanced multi-look processing model (Stenseng and Andersen 2012; Bao et al. 2013): improved resolution along the track by 20 times and improved accuracy in sea surface height measurements. The related products have been used to confirm and refine the positions of some tectonic boundaries (Sandwell et al. 2014a). However, this altimetry can not improve the accuracies in the directions of non along-track. Since the InSAR altimeter can observe two-dimensional elevation near the ground track (Bao et al. 2013; Sui et al. 2017); thus, compared with a traditional altimeter, it has great advantages in the calculation of the gravity gradient. It is expected that this could provide gravity gradient data that can meet the requirements of bathymetry inversion with high accuracy.

## Conclusions

In this paper, the sensitivity and accuracy requirements of the gravity anomalies and gravity gradient data for bathymetry inversion are analyzed and some numerical test results are provided. The results show that the gravity gradient is more sensitive to the high-frequency part of the seafloor topography than the gravity anomaly. In particular, for a topography inversion with accuracy of 100 m, the accuracy requirements are different for the gravity anomaly or the gravity gradient when the inversion resolution is different.

For the gravity anomaly, the higher the inversion resolution is, the higher the accuracy requirements are. The fundamental reason behind this is that the gravity anomaly signal generated by the high-frequency part of the terrain is relatively weak. In contrast, for the vertical gravity gradient, with an increase in the inversion resolution of the seafloor topography, the accuracy requirement of the gravity gradient first decreases and then increases, i.e. it is not monotonous. This shows that the vertical gravity gradient is more sensitive to the high-frequency part of the topography. In addition, the vertical gravity gradient has a band that is most sensitive to the seafloor topography, which is related to the depth and area size of the terrain.

The underlying theory suggests that the magnitude of the gravity anomaly and vertical gravity gradient noises should be smaller than those of the signals. However, for the actual seafloor topography inversion, we additionally need to consider the accuracy of the algorithm, such as non-linear error, separation error of the long and short wavelengths of the gravity signal or vertical gravity gradient signal and the error from density difference constant. In addition, from our analysis, products of the current satellites cannot satisfy requirements of bathymetry inversion completely. Therefore, new gravity satellites and altimetry satellites are needed to provide gravity anomalies and vertical gravity gradients with higher accuracy. The results of this study provide a reference for the design of the related satellites.

**Acknowledgements** This work is funded by the National Nature Science funds of China (Nos. 41674026, 41404019, 41506076), the open fund of Key Laboratory of Space Utilization, Chinese Academy of Sciences (CSU-WX-A-KJ-2016-044) and China Ocean Mineral Resources R&D Association project (S2-2-06).

## References

- Bao L, Hsu H, Li Z et al (2013) Towards a 1 mGal accuracy and 1 min resolution altimetry gravity field. *J Geodesy* 87:961–969
- Calmant S (1994) Seamount topography by least-squares inversion of altimetric geoid heights and shipborne profiles of bathymetry and/or gravity anomalies. *Geophys J Int* 119:428–452
- Calmant S, Baudry N (1996) Modelling bathymetry by inverting satellite altimetry data: a review. *Mar Geophys Res* 18:12–134
- Dixon T, Naraghi M (1983) Bathymetric prediction from SEASAT altimeter data. *J Geophys Res* 88:1563–1571
- Fu LL, Alsdorf D, Morrow R, Rodriguez E, Mognard N (2012) SWOT: the surface water and ocean topography mission. Academic Press, New York
- Hsiao Y, Kim J, Kim K, Lee BY, Hwang C (2011) Bathymetry estimation using the gravity-geologic method: an investigation of density contrast predicted by downward continuation method. *Terr Atmos Ocean Sci* 21(3):347–358
- Hsiao YS, Hwang C, Cheng YS, Chen LC, Hsu HJ, Tsai JH, Liu CL, Wang CC, Liu YC, Kao YC (2016) High-resolution depth and coastline over major atolls of South China Sea from satellite altimetry and imagery. *Remote Sens Environ* 176:69–83

- Hu M, Li J, Li H et al (2014a) Predicting global seafloor topography using multi-source data. *Mar Geodesy*. <https://doi.org/10.1080/01490419.2014.934415>
- Hu M, Li H, Shen C (2014b) A program for bathymetry prediction from vertical gravity gradient anomalies and ship soundings. *Arab J Geosci*. <https://doi.org/10.1007/s12517-014-1570-0>
- Hwang C (1998) Inverse vening meinesz formula and deflection-geoid formula: applications to the predictions of gravity and geoid over the South China Sea. *J Geodesy* 72(5):304–312
- Hwang C (1999) A bathymetric model for the south China Sea from altimetry and depth data. *Mar Geodesy* 22:37–51
- Ibrahim A, Hinze W (1972) Mapping buried bedrock topography with gravity. *Ground Water* 10:18–23
- Jena B, Swain D, Tyagi A et al (2012) Prediction of bathymetry from satellite altimeter based gravity in the Arabian sea: mapping of two unnamed deep seamounts. *Int J Appl Earth Obs Geoinf* 12:1–4
- Kim S, Wessel P (2015) Finding seamounts with altimetry-derived gravity data. In: *Proceedings of Oceans 2015: MTS/IEEE Washington*. <https://doi.org/10.23919/OCEANS.2015.7401883>
- Kim S, Wessel P (2016) New analytic solutions for modeling vertical gravity gradient anomalies. *Geochem Geophys Geosyst* 17:1915–1924. <https://doi.org/10.1002/2016GC006263>
- Kim KB, Hsiao YS, Kim JW, Lee BY, Kwon YK, Kim CH (2010) Bathymetry enhancement by altimetry-derived gravity anomalies in the East Sea (Sea of Japan). *Mar Geophys Res* 31(4):285–298
- Kim J, Frese R, Lee B, Roman DR, Doh SJ (2011) Altimetry-derived gravity predictions of bathymetry by gravity-geologic method. *Pure Appl Geophys* 168:815–826
- Molodensky MC (1960) *The gravity field and figure of the earth*. Tp. LIHNNTIHK 131
- Moritz H (2005) *Physical geodesy, second correction edition*. Springer, New York
- Ouyang M, Sun Z, Zhai Z (2014) Predicting bathymetry in south china sea using the gravity-geologic method. *Chin J Geophys* 57:2756–2765
- Proakis JG, Manolakis DG (2007) *Digital signal processing: principles, algorithms & applications, 3rd edn*. Prentice Hall, Upper Saddle River
- Rummel R, Haagmans RHN (1990) Gravity gradients from satellite altimetry. *Mar Geodesy* 14:1–12. <https://doi.org/10.1080/15210609009379641>
- Sandwell D, Smith W, Gille S, Jayne S, Soofi K, Coakley B (2001) *Bathymetry from space: white paper in support of a high-resolution, ocean altimeter mission*. Scripps Institution of Oceanography, San Diego, pp 1–54
- Sandwell D, Smith W, Gille S, Kappel E, Jayne S, Soofi K, Coakley B, Geli L (2006) Bathymetry from space: rationale and requirements for a new, high-resolution altimetric mission. *C R Geosci* 338(14–15):1049–1062
- Sandwell D, Muller R, Smith W, Richard F (2014a) New global marine gravity model from CryoSat-2 and Jason-1 reveals buried tectonic structure. *Science* 346(6205):65–67
- Sandwell D, Carcla E, Smith W (2014b) Recent improvements in Arctic and Antarctic marine gravity: unique contributions from CryoSat-2, Jason-1, Envisat, Geosat and ERS-1/2. *American Geophysical Union (AGU)*
- Smith W, Sandwell D (1997) Global sea floor topography from satellite altimetry and ship depth soundings. *Science* 277:1956–1962
- Stenseng L, Andersen O (2012) Preliminary gravity recovery from CryoSat-2 data in the Baffin Bay. *Adv Space Res* 50:1158–1163
- Sui X, Zhang R, Wu F, Li Y, Wan X (2017) Sea surface height measuring using InSAR altimeter. *Geodesy Geodyn*. <https://doi.org/10.1016/j.geog.2017.03.005>
- Wan X, Zhang R, Li Y, Liu B, Sui X (2017) Matching relationship between precisions of gravity anomaly and vertical deflections in terms of spherical harmonic function. *Acta Geod Cartogr Sin* 46(6):706–713
- Wang Y (2000) Predicting bathymetry from the Earth's gravity gradient anomalies. *Mar Geod* 23(4):251–258
- Wang Y, Xu H, Zhan J (2001) High resolution bathymetry of China seas and their surroundings. *Chin Sci Bull* 19:956–960
- Xiang X, Wan X, Zhang R et al (2017) Bathymetry inversion with gravity-geologic method: a study of long-wavelength gravity modeling based on adaptive mesh. *Mar Geodesy* 40(5):329–340. <https://doi.org/10.1080/01490419.2017.1335257>